The N-Terminal Fragment of Human Parathyroid Hormone Receptor 1 Constitutes a Hormone Binding Domain and Reveals a Distinct Disulfide Pattern

Ulla Grauschopf,[‡] Hauke Lilie,[‡] Konrad Honold,[§] Manfred Wozny,[§] Dietmar Reusch,[§] Angelika Esswein,[||] Wolfgang Schäfer,[||] Karl Peter Rücknagel,[⊥] and Rainer Rudolph*[,‡]

Institut für Biotechnologie der Martin-Luther-Universität Halle-Wittenberg, Kurt-Mothes-Strasse 3, D-06120 Halle, Germany, Roche Diagnostics GmbH Pharma Research Penzberg, Nonnenwald 2, D-83277 Penzberg, Germany, Roche Diagnostics GmbH, Sandhoferstrasse 116, D-68296 Mannheim, Germany, and Forschungsstelle "Enzymologie der Proteinfaltung" der Max-Planck-Gesellschaft, Weinbergweg 22, D-06120 Halle/Saale, Germany

Received January 21, 2000; Revised Manuscript Received May 12, 2000

ABSTRACT: The N-terminal extracellular parts of human G-protein coupled receptor class B, for example, receptors for secretin, glucagon, or parathyroid hormone, are involved in ligand binding. To obtain structural and functional information on the N-terminal receptor fragment of human parathyroid hormone receptor 1 (PTHR1), the truncated receptor was expressed in the cytosol of *Escherichia coli* in the form of inclusion bodies. Oxidative refolding of inclusion body material resulted in stable, soluble, monomeric protein. Ligand binding was proved by surface plasmon resonance spectroscopy and isothermal titration calorimetry. Refolded receptor fragment was able to bind parathyroid hormone with an apparent dissociation constant of 3−5 μM. Far-UV circular dichroism spectra showed that the refolded polypeptide contained approximately 25% α-helical and 23% β-sheet secondary structures. Analysis of the disulfide bond pattern of the refolded receptor fragment revealed disulfide bonds between Cys170 and Cys131, Cys148 and Cys108, and Cys117 and Cys48. These results demonstrate that the extracellular N-terminal domain of the parathyroid hormone receptor (PTHR1) possesses a well-defined, stable conformation, which shows a significant ligand binding activity.

Parathyroid hormone receptor (PTHR1),[1] as well as other receptors for peptide hormones such as secretin, pituitary adenylate cyclase activating polypeptide (PACAP), glucagon, glucagon-like peptide 1 (GLP1), and calcitonin, belong to class B of the G-protein-coupled receptors (*1*). Receptors of this class share sequence homology in their seven transmembrane spanning helices but are not homologous to other members of the G-protein-coupled receptor superfamily. Binding of polypeptide hormones to class B G-protein-coupled receptors controls fundamental processes such as bone turnover (PTH), insulin secretion (glucagon, GLP1), or regulation of neurosecretion (α-latrotoxin receptor) (*2, 3*). Like all other members of the class B receptor family, PTHR1 contains a large N-terminal domain with few highly conserved amino acid residues, including six cysteines. These cysteine residues are necessary for the ligand binding properties (*4*) and are assumed to form three disulfide bridges. Cross-linking and mutagenesis experiments as well as studies with chimeric receptors suggest that ligand binding and/or specificity resides primarily in the N-terminal part of the protein, whereas signal transduction to the cytosol occurs in the transmembrane domain (*5*−*8*).

Information on the molecular structure of the receptors and their ligand-bound complexes is of great pharmaceutical interest but is thus far not available. Such information would allow the development of improved receptor agonists and antagonists against a number of metabolic diseases such as osteoporosis (PTHR1) and diabetes (GLP1 receptor) by rational drug design. This lack of structural information is mainly due to the difficulties in the overexpression of the full-length receptors in expression systems that could be used for preparation of protein in suitable amounts (*9*) as well as to the purification and crystallization of multispanning membrane proteins. In a previous paper, NMR and molecular dynamic simulation were used to characterize a 31-amino acid residue synthetic peptide, PTHR1(168−198), which includes part of the first transmembrane helix and the adjacent extracellular amino acid residues (*10*). These and other authors proposed a binding model in which this peptide is involved in ligand binding, but other interaction points in the remaining N-terminus and the extracellular loops of PTHR1 are required for effective binding (*11*−*14*). To

* To whom correspondence should be addressed. Phone: +49-345/5524889. Fax: +49-345/5527013. E-mail: rudolph@biochemtech.uni-halle.de.

[‡] Institut für Biotechnologie der Martin-Luther-Universität Halle-Wittenberg.

[§] Roche Diagnostics GmbH Pharma Research Penzberg.

[||] Roche Diagnostics GmbH, Mannheim.

[⊥] Forschungsstelle "Enzymologie der Proteinfaltung" der Max-Planck-Gesellschaft.

[1] Abbreviations: CD, Circular dichroism; DTT, dithiothreitol; EDTA, ethylenediaminetetraacetate; GLP1, glucagon-like peptide 1; GSH, reduced glutathione; GSSG, oxidized glutathione; HIC, hydrophobic interaction chromatography; HPLC: high performance liquid chromatography; IMAC, immobilized metal affinity chromatography; IPTG, isopropylthiogalactoside; LDAO, *N*,*N*-dimethyldodecylamine *N*-oxide; nPTHR, N-terminal binding domain of the human PTH-receptor; PMSF, phenylmethanesulfonyl fluoride; PTH, parathyroid hormone; PTHR1, parathyroid hormone 1 receptor; SDS, sodium dodecyl sulfate; TCA, trichloroacetic acid; TRIS, Tris(hydroxymethyl)aminomethane.

10.1021/bi0001426 CCC: $19.00 © 2000 American Chemical Society
Published on Web 07/06/2000

initiate structural studies of the receptor−ligand interaction, we overexpressed the complete N-terminal, extracellular part of the PTHR1 in *Escherichia coli*. Starting with the assumption that this protein forms a globular, stable domain [as has been shown for a N-terminal domain of the GLP1 receptor (*15*) and the PACAP receptor (*16*)], this protein should allow analyses of ligand-binding properties. The N-terminal PTHR1 domain, nPTHR, was expressed and deposited as inclusion bodies in *E. coli*. After renaturation and purification were performed, we could confirm the functionality of the refolded protein in comparison to membrane-bound full-length PTHR1 and obtain structural information on the ligand binding domain, including the disulfide pattern.

EXPERIMENTAL PROCEDURES

Materials. (Ahx35,36; Cys37)-PTH-(1−37)-NH_2 was a gift from Eike Hoffmann (Roche Diagnostics GmbH). PTH(1−37) was kindly provided by Karlheinz Sellinger (Roche Diagnostics GmbH). All other chemicals were of analytical grade and obtained from major commercial suppliers.

Cloning and Expression of the N-Terminal Binding Domain of Human PTHR1. A 504-bp gene fragment, coding for amino acid residues 23−191 of the human PTHR1, was amplified by standard PCR techniques from a cDNA template encoding the complete receptor with primer 1 (5′-GGGAAACTTCATATGTACGCGCTGGTGGATG-CAG-3′) and primer 2 (5′-CACGGATCCTCATTAAAT-CATGCCCAGGGGTCAAACAC-3′). The PCR fragment was cloned into pET15b (Novagen) using *Bam*HI and *Nde*I restriction sites. The resulting recombinant expression vector, p(nPTHR), codes for the PTHR1 fragment, with an N-terminal His-tag. The authenticity of the PTHR1 fragment insert was confirmed by DNA sequence analysis of both strands.

For expression of nPTHR, the plasmid was transferred into the *E. coli* strain BL21(DE3). Since translation of eucaryotic transcription products in *E. coli* is often impaired by differences in codon usage, especially by the rare codons for L-arginine, AGA and AGG, we cotransfected the host cells with an additional plasmid, pUBS520, that enables constitutive expression of the corresponding tRNA (*17*, *18*). For shake flask growth, 1 L LB-medium supplemented with kanamycin (25 μg/mL) and ampicillin (100 μg/mL) was inoculated with 10 mL overnight culture and cultivation was performed at 37 °C. At an optical density of $OD_{546\ nm}$ = 0.8, protein expression was induced with 1 mM IPTG. After an additional 3 h incubation, cells were harvested by centrifugation (15 min; 4000*g*). For large scale production, we used a fed batch fermentation protocol according to Teich et al. with minor modifications (*19*). The fermentation was carried out in a 10 L Biostat ED bioreactor (B. Braun, Germany) with an initial culture volume of 8 L at 35 °C. Recombinant protein expression was induced 2 h after feeding start at an optical density of $OD_{500\ nm}$ = 60 by injection of 0.4 mM IPTG. After an additional 3 h, cells were harvested by centrifugation and stored at −20 °C.

Inclusion Body Preparation and Refolding. Twenty grams of cells were resuspended in 100 mL of 0.1 M TRIS and 1 mM EDTA, pH 7, and disrupted by high-pressure dispersion. After cell lysis was performed, 10 μg/mL DNAse I and 3 mM $MgCl_2$ were added, and the solution was incubated for 20 min at room temperature. After the solution was mixed with 0.5 vol of 0.1 M TRIS/HCl, 150 mM NaCl, and 1.5% LDAO at pH 7, insoluble material was collected by centrifugation (30 min; 30000*g*). The obtained pellet was resuspended in 0.1 M TRIS, 150 mM NaCl, pH 7, containing 0.5% LDAO. Followed by a second washing step, the washing procedure was repeated twice without LDAO. The collected inclusion bodies were stored at − 20 °C until use. After inclusion bodies were solubilized in 0.1 M TRIS, 6 M guanidinium chloride, 100 mM DTT, and 1 mM EDTA, pH 8 (10 mg of inclusion body material/mL), at room temperature for 2 h, insoluble material was removed by centrifugation (30 min; 30000*g*). To remove DTT, the solubilized protein was extensively dialyzed against 4 M guanidinium chloride and 0.1 M sodium phosphate, pH 6.

To obtain binding of the His-tagged protein to an IMAC column (Qiagen), the pH of the solution was readjusted to pH 8 by adding 1 M NaOH. After washing the column with 0.1 M sodium phosphate and 4 M guanidinium chloride, pH 6.3, nPTHR was eluted by a pH shift to pH 4.5. Renaturation was achieved by dialysis against 15 vol of renaturation buffer (1 M L-arginine, 0.05 M sodium phosphate, 1 mM EDTA, 5 mM GSH, and 1 mM GSSG, pH 8) at a protein concentration of 0.5−1 mg/mL for 4 days at 4 °C.

Protein Purification. Renatured protein was dialyzed against 1.5 M ammonium sulfate and 0.05 M sodium phosphate, pH 7.5. Aggregates were removed by centrifugation, and the protein solution was loaded onto a Phenyl Sepharose 6 Fast Flow (low sub) column (Pharmacia) for hydrophobic interaction chromatography (HIC). Elution was performed by a linear gradient of 1.5 M ammonium sulfate to 0 M ammonium sulfate in 0.05 M sodium phosphate, pH 7.5. Further purification was carried out on a gel filtration Superdex 75 prep grade column (Pharmacia) in 0.3 M ammonium sulfate and 0.05 M sodium phosphate, pH 7.5, at a flow rate of 1 mL/min. Protein concentration was determined spectrophotometrically using an absorption coefficient of $\epsilon_{280\ nm} = 37770\ M^{-1}\ cm^{-1}$, calculated according to Gill and von Hippel (*20*).

Analytical Ultracentrifugation. Sedimentation equilibrium measurements were performed in an analytical ultracentrifuge Optima XL-A (Beckman Instruments). Double sector cells were used at 20 000 rpm and 20 °C in an An60Ti rotor. Analyses were carried out at a protein concentration of 0.4 mg/mL in 50 mM potassium phosphate and 0.3 M KCl, pH 8.0. The data were analyzed with a program developed by Minton (*21*). For calculations, a partial specific volume of 0.734 mL/mg was assumed.

Chromatographic Analysis of Refolded nPTHR by Reversed Phase HPLC. Refolded and purified nPTHR (3 μg of protein in 50 mM sodium phosphate, 0.3 M NaCl, pH 7.5) was loaded onto a ET125 × 2 Nucleosil500-5 C3PPN (Macherey-Nagel) reversed-phase column, equilibrated in solvent A (0.09% TFA) at a flow rate of 200 μL/min and 40 °C. After a 2-min wash with 1% acetonitrile, the protein was eluted by a gradient versus solvent B (0.08% TFA in 80% acetonitrile).

Differential Scanning Calorimetry. Temperature scans were performed with a VP-DSC Micro calorimeter (MicroCal, Inc., Northampton, MA) at a protein concentration of 200 μg/mL in 50 mM sodium phosphate and 150 mM NaCl,

pH 7. Evaluation of the data was carried out with the manufacturer's software (MicroCal Origin 4.1).

Spectroscopic Techniques. CD spectra were recorded at 22 °C using an AVIV 62A DS spectropolarimeter (AVIV, Lakewood, NJ) in a 0.02-cm quartz cuvette. The spectra were accumulated 11 times with an average time of 7 s and a bandwidth of 1 nm. Spectra were recorded from 260 to 198 nm at a protein concentration of 18 μM in 0.05 M sodium phosphate and 0.3 M NaCl, pH 7.5, for the native protein, and from 260 to 210 nm at a protein concentration of 28 μM in 6 M guanidinium chloride for the unfolded protein. The spectra were corrected for buffer contributions and converted to mean residue weight ellipticity according to Schmid (*22*). For secondary structure analyses, the program CDNN was applied (*23*).

Disulfide Pattern Analysis. The protein was transferred into 0.1 M TRIS and 10 mM $CaCl_2$, pH 7.8, by dialysis (final protein concentration: 47 μg/mL). To 1 mL of the solution, 6 μL of a chymotrypsin solution (1 mg/mL of chymotrypsin in 1 mM HCl, chymotrypsin sequencing grade, Roche Molecular Diagnostics) were added. Subsequently, the protein was digested overnight at 37 °C. A total of 200 μL of the digestion mixture was injected into a microbore HPLC system (140A, Applied Biosystems, Foster City, USA) and separated by reversed-phase HPLC using a YMC ODS-AQ C 18 column (pore size 120 A, particle size 5 μm, length 25 cm, inner diameter 1 mm) and linear gradient elution (eluent A: 0.1% TFA in water; eluent B: 80% acetonitrile, 20% water, and 0.1% TFA; slope of the separating part of the gradient: 0.67% B/min; flow rate: 50 μl/min; column temperature: 35 °C).

For online monitoring of cyst(e)ine-containing peptides, a previously described methodology consisting of postcolumn derivatization with a reagent solution containing thiosulfonate and NTSB (*24*) was employed.

In the reaction mixture, disulfides (R^1SSR^2) are first cleaved by sulfitolysis:

$$R^1SSR^2 + SO_3^{2-} \rightarrow R^1SS0_3^- + R^2S^- \text{ (pH > 9)} \quad (1)$$

The detection is then based on the reaction of the thiolate anions R^2S^- with NTSB (2-nitro-5-thiosulfobenzoate):

$$NTSB + R^2S^- \rightarrow NTB + R^2SSO_3^- \text{ (pH > 9)} \quad (2)$$

The time available for reaction was approximately 1 min. The reaction product NTB (2-nitro-5-thiobenzoate) was detected spectrophotometrically at 432 nm.

A stock solution of NTSB was produced as follows: 10 g of DTNB [5,5′-dithiobis-(2-nitrobenzoate)] was dissolved in 800 mL of 1 M Na_2SO_3, pH 7.5 (adjusted with NaOH). The solution was heated to 38 °C, and oxygen was bubbled through it until the initially bright red solution had turned to a pale yellow. The final reagent solution was prepared by diluting the NTSB stock solution 1:10 with 50 mM glycine and 100 mM Na_2SO_3, pH 9.5 (adjusted with NaOH).

For disulfide elucidation, two HPLC runs were performed. One run included postcolumn derivatization (analytical run; detection at 220 and 423 nm). The second run, including fraction collection (volume of fractions: 50 μL), was performed without postcolumn reaction (collection run). The fractions containing cyst(e)ine were further analyzed by Edman sequencing (instrument: Procise, Applied Biosystems, Foster City, USA; 20 μL of the RP-HPLC eluent were loaded using ProSorb cartridges, Applied Biosystems).

Cross-Linking by Glutaraldehyde. nPTHR (1 μM in 50 mM sodium phosphate and 300 mM NaCl, pH 8.0) was incubated with PTH (10 μM) or insulin (10 μM) in the presence of 40 mM glutaraldehyde for 20 min at 4 °C. Sodium borohydride was added to a concentration of 43 mM, and the proteins were precipitated by 35% TCA. The precipitated protein was dissolved in SDS−PAGE sample buffer and analyzed by SDS−PAGE. As a control, nPTHR and PTH alone were subjected to the same procedure.

Surface Plasmon Resonance. Association and dissociation reactions of refolded nPTHR and human parathyroid hormone were studied by surface plasmon resonance in a BIAcoreX-System (BIAcore AB, Uppsala, Sweden). Coupling of PTH(1−34), which contained two aminohexane spacers and an additional cysteine residue at the C-terminus, to a CM5 sensor chip was performed via thiol-coupling according to the manufacturer's instructions. The derivatization levels were between 300 and 500 resonance units. Different concentrations of 50 μL nPTHR in 50 mM TRIS/HCl, 100 mM NaCl, 5 mM KCl, 2 mM $CaCl_2$, and 2 mM $MgCl_2$, pH 7.5, were injected over the two flow cells at a flow rate of 20 μL/min. While one flow cell was coated with PTH(1−34), the other one was blocked with cysteine. Regeneration of the chip surface was achieved by injection of 50 μL of 0.2% SDS and 50 μL of 6 M urea and 0.1 M glycine, pH 2.5, which resulted in no loss of activity of the coupled ligand. Data analysis was performed by fitting the nPTHR concentration versus the plateau values obtained after completion of the association reaction according to the Langmuir binding isotherm. Competition experiments were done by preincubation of 1 μM nPTHR with different concentrations of PTH. The amount of free receptor was analyzed by its ability to bind to the PTH sensor chip. Calculations of the dissociation constant was performed according to eqs 3 and 4. with S as the measured resonance

$$S = S_0 + \left(\Delta S_{max} \times \frac{(RL)}{(R_0)}\right) \quad (3)$$

signal after reaching the equilibrium plateau, S_0 as the resonance signal without competing peptide, ΔS_{max} as the difference between S_0 and S in the presence of a saturating concentration of competing peptide, and (RL) and (R_0) as the concentrations of receptor−ligand complex and total receptor, respectively. According to the law of mass action, the concentration of receptor−ligand complex is

$$(RL) = \frac{[(R)_0 + (\text{ligand})_0 + K_d]}{2} - \sqrt{\left\{\frac{[(R)_0 + (\text{ligand})_0 + K_d]}{2}\right\}^2 - R_0 \times (\text{ligand})_0} \quad (4)$$

Isothermal Titration Calorimetry. Isothermal titration calorimetry experiments were carried out using a MicroCal ITC titration calorimeter (MicroCal, Inc., Northampton, MA) using procedures previously described (*25*). A series of injections of PTH (600−700 μM) into a nPTHR solution (20−25 μM) were carried out. All measurements were

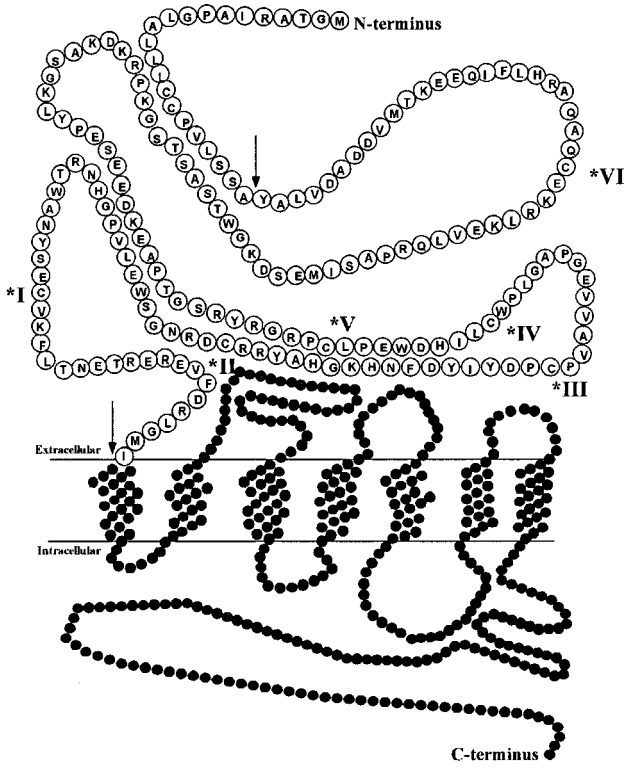

FIGURE 1: Schematic presentation of the human PTH receptor 1. The primary structure of the extracellular N-terminal part of PTHR1 is shown. nPTHR is marked by arrows, and the conserved cysteines are indicated by asterisks. Boundaries of the transmembrane segments TM-I to TM-VII are based on ref *53*.

performed at 20 °C in 50 mM TRIS/HCl, 100 mM NaCl, 5 mM KCl, 2 mM $CaCl_2$, and 2 mM $MgCl_2$, pH 8.0. The data were analyzed with ORIGIN software (Microcal Software, Northampton, MA).

RESULTS

Expression and Refolding of the nPTHR. As the N-terminal extracellular part of the receptor, nPTHR, is assumed to be involved in binding of PTH (*5*, *11*−*13*, *26*), we established a system for recombinant production of this receptor fragment for structural studies and in vitro characterization of ligand−receptor interaction. The first 22 amino acids of PTHR1 consists of a signal sequence that is not present in the mature protein. Tyr23 was determined to be the N-terminal amino acid residue of the in vivo processed receptor (data not shown). According to a prediction using the PHDhtm Predict Protein algorithm (*27*), the amino acid Ile191 is directly connected to the first transmembrane helix. Thus, Ile191 was chosen as the C-terminus of the fragment. A cDNA encoding nPTHR (Tyr23−Ile191, Figure 1) was amplified via PCR and inserted in a pET15b vector (Novagen).

nPTHR was expressed in *E. coli* with a yield of 10−15% of the total protein of an *E. coli* extract (Figure 2). SDS−polyacrylamide gel electrophoresis of soluble and insoluble protein fractions showed that nPTHR was deposited almost exclusively in inclusion bodies. After cell disruption, the inclusion bodies were collected and purified by washing the insoluble fraction with 0.5% LDAO. As shown in Figure 2, this fraction shows a high content of nPTHR.

To obtain native protein, a refolding procedure was developed. Prior to renaturation, the solubilized and reduced

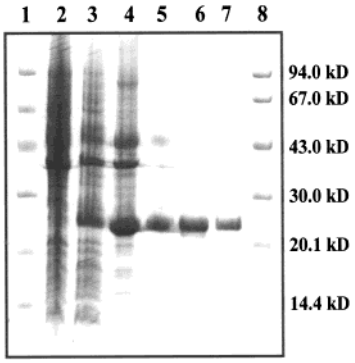

FIGURE 2: SDS−PAGE of bacterial extracts and nPTHR. SDS−PAGE was carried out according to Schägger and Jagow (*54*) with a 12% polyacrylamide gel. Lanes 1 and 8, molecular mass marker proteins; lane 2, bacterial proteins obtained before induction; lane 3, cell lysate 3 h after induction; lane 4, insoluble protein fraction (inclusion bodies); lane 5, guanidinium chloride solubilized inclusion body proteins after purification on Ni-NTA; lane 6, protein fraction after renaturation and hydrophobic interaction chromatography; lane 7, pooled fractions of nPTHR after gel filtration.

inclusion bodies were purified by IMAC (Figure 2, lane 5). For renaturation, the eluted protein was dialyzed against renaturation buffer (1 M L-arginine, 1mM EDTA, 5 mM GSH, 1 mM GSSG, and 0.05 M sodium phosphate, pH 8) for 4 days at 4 °C at protein concentration of 0.5−1 mg/mL. During renaturation, the presence of high molar concentrations of L-arginine as a solubilizing agent was essential. In the absence of L-arginine, no renaturation could be observed at these protein concentrations. The necessity of a redox system present in the renaturation buffer was a first indication that disulfide bond formation is essential for structure formation. After renaturation, the protein solution was dialyzed against 1.5 M ammonium sulfate and 0.05 M sodium phosphate, pH 7.5, and aggregates were removed by centrifugation. Hydrophobic interaction chromatography (HIC), which is an appropriate method to separate protein isomers of different hydrophobicity, was performed to purify correctly folded protein from incorrectly folded species and impurities. The protein solution was loaded onto a Phenyl Sepharose 6 Fast Flow (low sub) (Pharmacia) and elution was carried out by decreasing the ammonium sulfate concentration. As shown in Figure 2, lane 6, the main peak contained nPTHR in almost homogeneous form. In a last purification step, gel filtration was performed. The purity of the protein was ≈95% as determined by SDS−polyacrylamide gel electrophoresis (Figure 2, lane 7). The final yield after renaturation and purification was approximately 30−50% of the initial solubilized inclusion body protein material.

Biochemical and Biophysical Characterization of the Refolded Receptor Fragment. Matrix-assisted laser desorption/ionization mass spectroscopy and automated Edman degradation confirmed the identity and the molecular mass of 21.496 kD of the refolded receptor fragment (data not shown). All cysteines of the protein participate in disulfide bond formation since no free thiol groups could be detected by an assay using Ellman's reagent (*28*).

The homogeneity of disulfide bonding of the refolded, purified protein was confirmed by reversed-phase HPLC (Figure 3). This result indicated that upon renaturation disulfide bond formation was not a statistical process but guided by a defined secondary and tertiary structure.

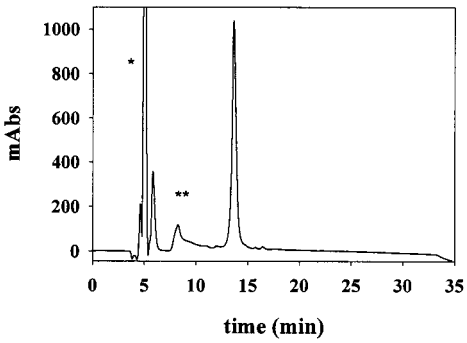

FIGURE 3: Reversed-phase HPLC of the refolded nPTHR. Approximately 3 μg nPTHR were loaded onto a ET125 × 2 Nucleosil500−5 C3PPN (Macherey-Nagel) reversed-phase column. After a washing step (2 min, 1% acetonitrile), the protein was eluted in a gradient from 30 to 80% acetonitrile (solvent A: 0.09% TFA; solvent B: 0.08% TFA in acetonitrile). The protein eluted as a single peak at 13.63 min. Peaks at 5 min (*) and 8 min (**) corresponded to PMSF and the gradient step, respectively.

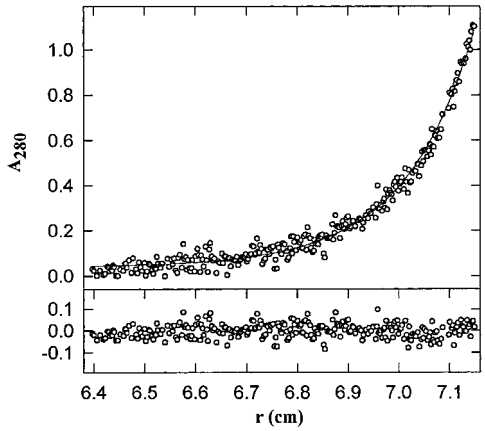

FIGURE 4: Molecular mass determination of nPTHR. Molecular mass of nPTHR was determined by analytical ultracentrifugation. The protein concentration was 0.4 mg/mL in 50 mM potassium phosphate and 0.3 M KCl, pH 7.5. Sedimentation equilibrium was measured at 20 000 rpm and 20 °C. Upper panel: absorbance data (o) were fitted to a single species of 20 810 Da (−). Lower panel: deviation of the fit to the experimental data.

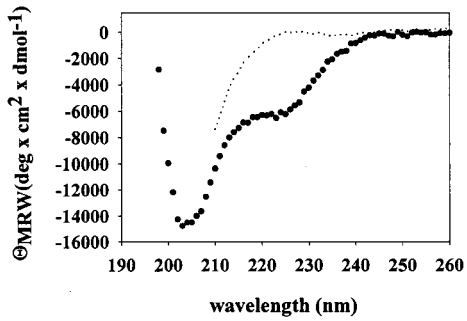

FIGURE 5: CD spectrum of nPTHR. CD spectra of a 18 μM solution of native nPTHR (•••) in 0.05 M sodium phosphate and 0.3 M NaCl, pH 7.5, were obtained as described under Experimental Procedures. For measuring spectra of the unfolded protein (···), a 28 μM solution in 6 M guanidium chloride was prepared. A 25% α-helical and 23% β-sheet structure was calculated for the native protein using the CDNN program (*23*).

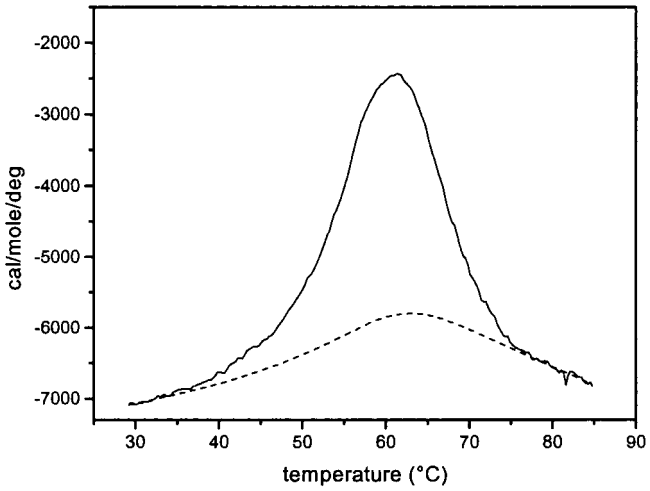

FIGURE 6: Differential scanning calorimetry with nPTHR. Temperature scans at a scan rate of 60 °C/h were performed from 7 to 85 °C at a protein concentration of 13 μM in 50 mM sodium phosphate and 150 mM NaCl, pH 7.0. Experimental data were analyzed using MicroCal ORIGIN software, yielding a T_m of 61 °C and a $\Delta H_{unfolding}$ of 52 kcal/mol. The dashed line constitutes the calculated baseline.

Furthermore, using analytical ultracentrifugation the refolded protein was shown to be monomeric with a molecular mass of 20.8 kD (Figure 4).

To obtain structural information of refolded nPTHR, secondary structure elements were analyzed by far-UV−CD under native and denaturing conditions (Figure 5).

The spectrum of nPTHR under native conditions clearly indicated a high content of secondary structure. Using the program CDNN (*23*), we estimated the content of secondary structure to be 25% α-helix and 23% β-strand. Differential scanning calorimetry (Figure 6) revealed a thermal unfolding transition at 61 °C with an apparent $\Delta H_{unfolding}$ of 52 kcal/mol. Taken together, these data indicate that the refolded protein forms a homogeneous, monomeric and stable domain with defined secondary and tertiary structures.

Analysis of the Disulfide Pattern. Within the class B of G-protein-coupled receptors, extracellular cysteine residues are highly conserved. This fact leads to the assumption of a conserved disulfide bond pattern, which might be essential for structural integrity and functionality.

This hypothesis is confirmed by the loss of ligand binding observed under reducing conditions or upon removal of the cysteine residues by mutagenesis, as shown for the PTHR1 (*4*, *29*). To determine the disulfide pattern of refolded nPTHR, a protein digest with chymotrypsin was performed, and the resulting fragments were analyzed by RP-HPLC and N-terminal sequencing.

Figure 7 illustrates the RP-HPLC diagrams obtained for the analytical run [detection at 220 and 432 nm, including online postcolumn derivatization for cyst(e)ine detection] and the collection run (detection at 220 nm, including fraction collection) of a chymotryptic digest of the nPTHR sample. Cyst(e)ine-containing peptides, i.e., peptides exhibiting 432 nm signals, were only observed at retention times above 60 min. The cyst(e)ine-containing fractions were subjected to 10−13 cycles of automated Edman sequencing. In each fraction, the amino acid yields of the different sequencing cycles was tested for the presence of nPTHR amino acid sequences. The data could be fully explained by the nPTHR amino acid sequences shown in Table 1. The cleavage sites observed are in agreement with the known specificity of chymotrypsin (cleavage predominantly at the C-terminus of aromatic and hydrophobic amino acids). In addition to the

Table 1: Edman Sequencing of Cyst(e)ine Containing Fractions of the Collection Run Shown in Figure 6[a]

Fraction #	Number of Sequencing Cycles	nPTHR Amino Acid Sequences Determined [1)]	Amount [2)] (pmol)	Interpretation [3)]
32	10	Y|-LVDADD-MT	3	ALVDADDVMT...
		L|-APGEVVAVP	**1.5**	**C_{131}-C_{170}** disulphide linkage between
		Y|-E-VKF	**1.5**	GAPGEVVAVP**C_{131}**... and SE**C_{170}**VKF
		H|-AQAQ-E-R	**2**	**C_{48}-C_{117}** disulphide linkage between
		L|-WPL	**2**	RAQAQ**C_{48}**E... and **C_{117}**WPL
33	12	L|-APGEVVAVP-P	**3.5**	**C_{131}-C_{170}** disulphide linkage between
		Y|-E-VK	**3**	GAPGEVVAVP**C_{131}**P... and SE**C_{170}**VK... or
		W|-NY-E	**0.5**	ANYSE**C_{170}**...
34	10	L|-APG-VVAVP	**1**	**C_{131}-C_{170}** disulphide linkage between
		Y|-E—VK	**1**	GAPGEVVAVP**C_{131}**... and SE**C_{170}**VKF
		Y|-GRP-LPE	**1**	**C_{108}-C_{148}** disulphide linkage between
		Y|-R-DRNGS	**1**	RGRP**C_{108}**LPE... and RR**C_{148}**DRNGS...
		Y|-LVDADD	0.5	ALVDADD...
		Y|-FNHK	1	DFNHK...
35	12	Y|-LVDADDVMTKE	2	ALVDADDVMTKE...
		Y|-GRP-LPE	**2**	**C_{108}-C_{148}** disulphide linkage between
		Y|-R-DRNGS	**2**	RGRP**C_{108}**LPE... and RR**C_{148}**DRNGS...
		L|--PG-V-A	**0.5**	**C_{131}-C_{170}** disulphide linkage between
		Y|-E—-KF	**0.5**	GAPGEVVAVP**C_{131}**... and SE**C_{170}**VKF
36	10	V|-VP-PDYIY	**1.5**	**C_{131}-C_{170}** disulphide linkage between
		Y|-E-VKF	**1.5**	AVP**C_{131}**PDYIY... and SE**C_{170}**VKF
		Y|-GRP-LPE-D	**2**	**C_{108}-C_{148}** disulphide linkage between
		Y|-R-DRNGS	**2**	RGRP**C_{108}**LPEWD... and RR**C_{148}**DRNGS...
39	12	L|-APGEVVAVP-P	**4**	**C_{131}-C_{170}** disulphide linkage between
		Y|-E-VKF	**4**	GAPGEVVAVP**C_{131}**P... and SE**C_{170}**VKF
40	12	L|--PGEVVAVP-P	**4**	**C_{131}-C_{170}** disulphide linkage between
		Y|-E—VKF	**4**	GAPGEVVAVP**C_{131}**P... and SE**C_{170}**VKF
		Y|-LVDADDVMTKE	8	ALVDADDVMTKE...
43	13	L|--PGEVVAVP-PD	**1.5**	**C_{131}-C_{170}** disulphide linkage between
		Y|-E-VKF	**2.5**	SE**C_{170}**VKF and GAPGEVVAVP**C_{131}**PD... or
		L|-WPLGAPGE-VAV	**1**	**C_{117}**WPLGAPGEVVAVP**C_{131}**..., peptides containing C_{48} not detected
45	10	L|--PGEVVAVP	**1.5**	**C_{131}-C_{170}** disulphide linkage between
		Y|-E-VKF	**2.5**	SE**C_{170}**VKF and GAPGEVVAVP**C_{131}**... or
		L|-WPLGAPGE-	**1**	**C_{117}**WPLGAPGEVVAVP**C_{131}**..., peptides containing C_{48} not detected

[a] For details of the interpretation of the data, see text. [b] (Designated as footnote 1 in table): (-) determination of amino acid is not possible due to background, carry-over from previous cycle, presence of amino acid with low detection efficiency, or presence of cysteine; (X|) X indicates the amino acid preceding the sequence determined. [c] (Designated as footnote 2 in table): as estimated from the initial yield of the corresponding amino acid sequence, bold numbers correspond to disulfide-linked peptides. [d] (Designated as footnote 3 in table): (...) C-terminus is not defined by the sequencing results.

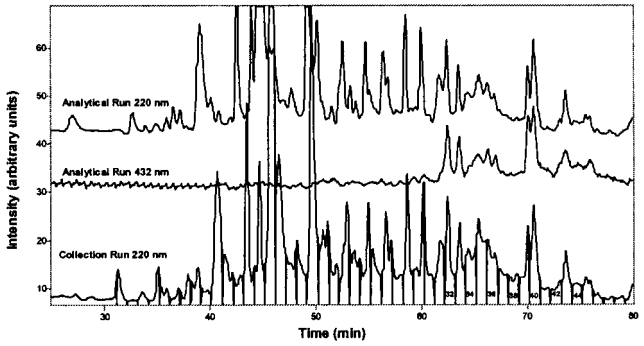

FIGURE 7: Disulfide pattern analysis of nPTHR. RP chromatograms obtained for the analytical run (detection at 220 nm before postcolumn reaction and at 432 nm after the cyst(e)ine-specific reaction) and the collection run (fractions collected without post-column reaction) of the chymotryptic digest of a nPTHR sample. The 432-nm chromatogram was multiplied by 10 to facilitate comparison. Cyst(e)ine-containing fractions were collected and further analyzed by automated Edman sequencing and electrospray mass spectrometry.

amino acid sequences, Table 1 also contains the amounts of peptides as estimated from the initial yields of the corresponding amino acid sequences. In fraction 39, only two peptides of comparable intensity exhibiting large differences in size and hydrophobicity were detected. Together with the intense cyst(e)ine signal of the fraction, this observation clearly indicates the existence of a disulfide linkage between Cys131 and Cys170. The same conclusion holds true for the data of fraction 40, since the amount of the peptide starting with the amino acid sequence ALV... significantly exceeds the amount of the remaining peptides. In addition, the nPTHR sequence following the sequence determined contains the sequence ...FLL$_{41}$... that constitutes a multiple cleavage site for chymotrypsin. Therefore, the C-terminus of the peptide starting with ALV... is unlikely to extend beyond Leu41 and to contain a cysteine residue. In contrast to the fractions 39 and 40, in the remaining fractions, more than two cysteine-containing peptides were detected. However, the data shown above demonstrate that the nPTHR molecule is structurally homogeneous. Strong evidence for the homogeneity of the disulfide pattern is in particular presented by the homogeneous reversed-phase chromatographic profile of the nPTHR sample. If the homogeneity of the disulfide pattern is taken

into account, the evaluation of the data of the remaining fractions unambiguously leads to the assignments given in the last column of Table 1. Therefore, besides the disulfide linkage between Cys131 and Cys170, further disulfide linkages of the nPTHR molecule are formed between Cys48 and Cys117 and between Cys106 and Cys146. The interpretation of the data given in Table 1 is supported by the fact that the amounts determined by Edman sequencing for the different peptides are consistent with the assignment of the disulfide linkages. Furthermore, the 432 nm peak intensities of the analytical run are in agreement with the amounts of cystine found in the different fractions by Edman sequencing. In addition, no free thiol could be detected in the sample using Ellman's reagent, i.e., all the cysteines are involved in disulfide linkages. However, the summed amounts of peptides corresponding to each of the three different disulfide linkages are significantly different (Cys48−Cys117: 4 pmol; Cys108−Cys148: 5 pmol; Cys131−Cys170: 19 pmol). This observation does not necessarily indicate the existence of alternative disulfide linkages. Since the degree of completeness of cleavage observed is rather limited (indicated for example by the large number of peptides connected by the disulfide linkage Cys131−Cys170), the lack of recovery of peptides connected by the disulfide linkages Cys48−Cys117 and Cys108−Cys148 is rather assumed to be due to limited cleavage of the peptide chain between Cys108 and Cys117. The lack of cleavage between Cys108 and Cys117 leads to the formation of complexes comprising four peptides connected by two disulfide linkages (Cys48−Cys117 and Cys108−Cys148) whose increased hydrophobicity may be responsible for the low recovery observed.

To check the results obtained by sequencing, we analyzed the major disulfide-containing fractions also by mass spectroscopy. To this end, the fractions 32, 39, and the pool of fraction 35 and 36 were rechromatographed, respectively. The resulting peaks were then analyzed by mass spectroscopy. For fraction 39, a single peak was detected with a peptide of a mass of 2196.29 Da. This corresponds to the disulfide bonded peptides (C131−C170) GAPGEVVAVPCPDYI and SECVKF (theoretical mass 2196.04 Da). Reduction of this peptide prior to mass spectroscopic analysis yielded a mass of 1486.41 Da for the peptide GAPGEVVAVPCPDYI; the other peptide was too small to be detectable. Rechromatography of fraction 32 resulted in three detectable peaks. One of these peaks was caused by the noncysteine-containing peptide ALVDADDVMTKEEQIFLL (2049.35 Da). The second peak consists of the above-mentioned disulfide-bonded dipeptide shortened by the C-terminal amino acid Ile (2082.84 Da). The third peak contained a peptide with a mass of 1320.70 Da. N-terminal sequencing identified this species as the disulfide-bonded dipeptide (C48−C117) RAQAQCE and CWPL (theoretical mass of 1320.58 Da).

Using mass spectroscopy, disulfide-bridged peptides comprising the third disulfide bond could not be identified unequivocally. This might be due to the heterogeneity in the N- and C-termini of the respective peptides, thus leading to a variety of peptides with different masses. However, all other biophysical data presented, including the lack of free cysteines and mixed disulfides, respectively, clearly prove the structural and functional homogeneity (see below) of

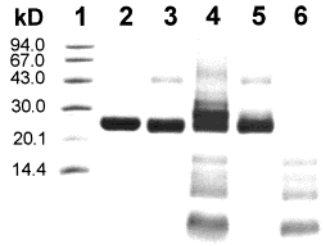

FIGURE 8: Cross-linking of nPTHR to PTH. nPTHR (1μM) was incubated with PTH (10 μM) or insulin (10 μM) in the presence of 40 mM glutaraldehyde for 20 min at 4 °C. Sodium borohydride was added to a final concentration of 43 mM, and the proteins were precipitated with 35% TCA and analyzed by SDS−PAGE. As a control, nPTHR and PTH alone were treated by the same procedure. Lane 1, molecular mass marker proteins; lane 2, nPTHR without cross-linker; lane 3, nPTHR with cross-linker; lane 4, 1μM nPTHR and 10 μM PTH with cross-linker; lane 5, 1 μM nPTHR and 10 μM insulin with cross-linker; lane 6, 10 μM PTH with cross-linker.

nPTHR, thus strongly suggesting that the two remaining cysteines form the disulfide bond C108−C148.

Binding Studies with Human Parathyroid Hormone. Glutaraldehyde-mediated cross-linking of nPTHR to PTH shows a distinct cross-link product by SDS−PAGE analysis in the appropriate size of a nPTHR−PTH complex (Figure 8) with a greater than 50% cross-linking efficiency. In a control reaction with insulin, another peptide hormone, no cross-link product could be detected. To exclude the possibility of the observed complexes being protein multimers, controls were also performed with nPTHR and PTH alone. In these control reactions, no cross-link product of appropriate size was detectable. These data, although qualitative, indicated a specific interaction of PTH with the refolded fragment nPTHR.

To determine the dissociation constant of refolded nPTHR with respect to ligand binding, surface plasmon resonance measurements were carried out. A modified parathyroid hormone peptide containing an additional cysteine at the C-terminus was used as a ligand. PTH was coupled to the sensor chip surface via the C-terminal cysteine. Unspecific binding to the modified sensor surface was not observed upon injection of a refolded N-terminal fragment of human GLP1 receptor, another member of the class B of G-protein-coupled receptors (*30*). In contrast, binding was observed upon injection of different concentrations of refolded nPTHR (Figure 9A). The plateau values reached after completion of the association reaction could be analyzed by a Langmuir binding isotherm (Figure 9B). We determined an apparent dissociation constant of 4.89 μM in 50 mM TRIS/HCl, 100 mM NaCl, 5 mM KCl, 2 mM $CaCl_2$, and 2 mM $MgCl_2$, pH 7.5. In another approach, competition experiments were carried out by preincubations of nPTHR with increasing concentrations of PTH(1−37). The remaining uncomplexed receptor fragment was again monitored by surface plasmon resonance. Figure 9C shows the decrease of the equilibrium plateau values with increasing competitor concentrations. Data analysis was carried out by nonlinear regression, which gave a dissociation constant of 3.38 μM.

A third method used to quantitatively assess the binding of PTH to nPTHR was isothermal titration calorimetry. Titration of PTH with nPTHR leads to the release of heat upon binding (Figure 10A). The analysis of the data (Figure 10B) revealed a 1:1 stoichiometry of the two binding

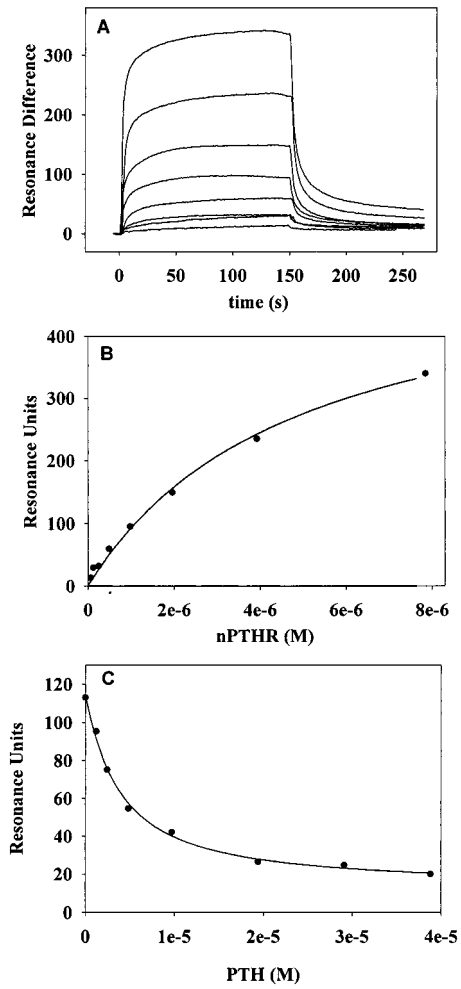

FIGURE 9: Ligand binding assays of the refolded nPTHR by surface plasmon resonance. PTH(1−34)-ligand was covalently attached via an additional C-terminal cysteine residue to a Biacore CM5 sensor chip. (A) Sensorgram shows the binding of (from bottom to top) 0.0615, 0.123, 0.25, 0.49, 0.981, 1.962, 3.925, and 7.85 μM nPTHR in 50 mM TRIS/HCl, 100 mM NaCl, 5 mM KCl, 2 mM $CaCl_2$, and 2 mM $MgCl_2$, pH 7.5, at a flow rate of 20 μL/min and 20 °C. (B) Plateau values were plotted against the nPTHR concentrations. To obtain the apparent dissociation constant, data points were fitted according to the Langmuir binding isotherm. (C) Competition experiments were carried out by preincubation of various concentrations of free PTH with 1 μM nPTHR before injection onto the sensor surface. Measured plateau values with respect to the competitor concentration are shown in 9C. Dissociation constants obtained were 4.9 and 3.4 μM for saturation binding experiments and competition experiments, respectively.

partners, a K_d value of 3.4 μM, and an apparent ΔH_{ITC} of −16.35 kcal/mol. Clearly, refolded nPTHR binds to its ligand in a specific manner, suggesting that the isolated, soluble fragment of PTH1R adopts a similar conformation as in the context of the full-length receptor.

DISCUSSION

Human PTHR1 belongs to a class of G-protein-coupled receptors, which bind short polypeptide ligands in the nanomolar range (*31*). Interaction of parathyroid hormone and parathyroid hormone related peptide with their receptors control calcium and phosphate homeostasis (*32*). Analyses of receptor−ligand interaction and elucidation of the structure of the ligand receptor complex will facilitate the rational design of low molecular weight receptor agonists or antagonists with considerable therapeutic potential (*33*). However, up to now, it has been impossible to obtain sufficient amounts of purified PTHR1 from natural sources or by recombinant expression for structural analyses. Mutagenesis and cross-linking experiments indicate that in addition to the N-terminal domain (*12*, *13*), ligand binding requires residues within the extracellular loops and transmembrane segments (*4*, *11*, *14*, *34*), but detailed structure/function analyses have not been carried out.

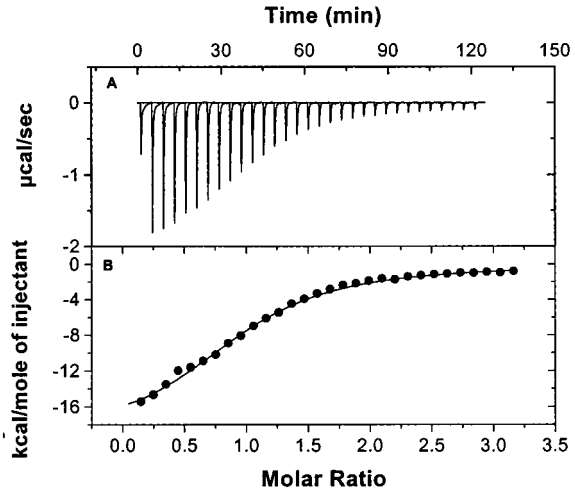

FIGURE 10: Isothermal Titration Calorimetry with nPTHR and PTH. A representative binding isotherm for binding of parathyroid hormone to nPTHR in 50 mM TRIS/HCl, 100 mM NaCl, 5 mM KCl, 2 mM $CaCl_2$, and 2 mM $MgCl_2$, pH 7.5, at 20 °C is shown. Top: baseline subtracted raw data. Bottom: peak-integrated and concentration-normalized enthalpy change vs PTH/nPTHR ratio. The solid line is the best fit to the experimental data according a 1:1 binding model. Averaging the best fit parameters of three independent measurements yields $K_d = 3.4$ μM; number of binding sites $N = 1.04$ and $\Delta H_{ITC} = 16.35$ kcal/mol.

Comprehensive biophysical studies of the structure/function relationship clearly demand sufficient amounts of protein in homogeneous form. To initiate a study on the receptor characteristics, the N-terminal domain of PTHR1 was expressed in *E. coli* leading to inclusion body formation. The deposition of a heterologously expressed protein in *E. coli* is a common phenomenon (*35*). Aggregation is most prominent when the recombinant protein contains disulfide bonds in its native state. In the last years, several procedures have been developed for restoration of the functional, native conformation of these proteins from the inclusion body material (*36*).

To refold nPTHR, which contains three putative disulfide bridges in the native functional form, we used reduced and oxidized glutathione as an oxido-shuffling system and L-arginine as a low molecular weight folding enhancer. This agent was shown to be very effective in other refolding protocols, including an extracellular domain of a Torpedo nicotinic acetylcholine receptor α-subunit (*37*), the human tissue-type plasminogen activator (*38*), and antibody Fab fragments (*39*). L-Arginine stabilizes the native state of a protein by preferential hydration (*38*, *40*), and it reduces unproductive aggregation of unfolded polypeptides or of folding intermediates by increasing their solubility during folding (*41*). As an oxido-shuffling system a 5:1 ratio of reduced GSH to oxidized GSSG was used, which allows rapid reshuffling of incorrect disulfide bonds (*42*). Using this

protocol, the yield of renaturation from inclusion body material was in a range of 30−50%. The refolded nPTHR was demonstrated to be a structurally well-defined, monomeric, stable protein.

Surface plasmon measurements and isothermal titration calorimetry confirmed the specific ligand binding properties of nPTHR. The dissociation constants determined by surface plasmon resonance studies were 4.9 and 3.4 μM for saturation binding experiments and competition experiments, respectively. The slight difference in K_d between binding and competition is probably due to the restricted mobility of the coupled PTH on the sensor surface. Isothermal titration calorimetry confirmed the dissociation constant of 3.4 μM and the proposed 1:1 binding stoichiometry. In comparison to membrane-bound full-length PTHR1, which binds PTH with a dissociation constant of 0.5 to 5 nM (*43*, *44*), we obtained decreased affinities for the refolded fragment. Different explanations that are not mutually exclusive could account for this lower affinity for PTH: (i) Previous studies indicated that ligand binding requires besides the N-terminal domain additional binding regions, located in the extracellular loops and the transmembrane regions (*14*, *45*). The absence of these additional interactions, provided only by the complete receptor molecule, might explain the lower binding affinity of the refolded nPTHR to its ligand. We are currently testing this hypothesis. (ii) The affinities of G-protein-coupled receptors are in some cases dependent on the coupling of heterotrimeric G proteins (*46*) as shown for the somatostatin receptor (*47*) and the latrotoxin receptor (*48*). The absence of such a mediator protein in our experiments could lead to a lower affinity of nPTHR for parathyroid hormone. (iii) A theory of structure induction of peptide hormones by hydrophobic preadsorption to the target cell membrane followed by the specific interaction with the receptor has been proposed (*49*, *50*). As our experiments were carried out in the absence of membranes, this structure induction cannot take place in our system and could lower the effective concentration of active parathyroid hormone in the ligand binding studies. (iv) Since nPTHR is expressed in a prokaryotic host, it lacks glycosylation, which could have an influence on binding affinity. However, it is thought that glycosylation plays only a minor role in the agonist binding of most G-protein-coupled receptors, although it may be important in determining the correct distribution of the receptor in the cell and in controlling receptor expression (*51*). Tunicamycin-induced inhibition of N-glycosylation was shown to have no effect on the function of β_2-adrenergic receptors (*52*) and of PTHR1 (*55*). (v) Renaturation of nPTHR could lead to a conformation that is a priori not able to bind PTH but instead is in equilibrium with a binding-competent conformation. Such an equilibrium would significantly raise the apparent dissociation constant. However, this explanations seems very unlikely. The well-defined disulfide pattern of the renatured protein indicates a clearly defined secondary and tertiary structure. Furthermore, no structural changes of nPTHR upon binding of PTH could be observed, neither by CD spectroscopy nor with differential scanning calorimetry (data not shown). Thus, our results clearly demonstrate that the domain is able to fold into a native-like conformation independently of the residual parts of the protein.

Secondary structure determination of refolded nPTHR by CD spectroscopy indicated a stable, folded structure with an α-helix content of 25% and β-sheet structure of 23%. Elucidation of nPTHR structure on an atomic level can now be performed by either X-ray analysis or NMR spectroscopy. NMR data have been so far obtained for a 31 amino acid residues synthetic fragment of the PTHR N-terminus, comprising residues 168−98 (*10*). The structure of this fragment, which in the full-length receptor represents the link between the N-terminus and the first transmembrane helix, is characterized by three α-helices, separated by a well-defined turn and a flexible region, as determined in a micellar solution of dodecylphosphocholine to mimic the membrane environment. The C-terminal helix is part of transmembrane helix I of the full-length receptor. Our secondary structure measurements of refolded nPTHR indicated besides α-helices a considerable amount of β-sheet structure. Comparison of other N-terminal fragments of G-protein-coupled receptors revealed that generally a substantial amount of β-sheet structure is present in these proteins (*37*).

The disulfide pattern of the refolded fragment revealed the connectivity of the conserved cysteine residues in the N-terminal part of the receptor. All receptors of this class contain these conserved residues. Data obtained with the refolded N-terminal domain of the human GLP1-receptor show the same disulfide bond pattern as found in nPTHR (Bazasuren, A. et al., unpublished results). Therefore, we propose a common disulfide pattern in this family of receptors in which cysteine residues I and III, II and V, and IV and VI, starting with the C-terminus of nPTHR[2] are connected.

Our results show the feasibility of overexpression of the N-terminal ligand binding domain of class B G-protein-coupled receptors and its subsequent refolding to a functional protein domain. The approach chosen provides large amounts of protein for both structural and ligand-binding studies.

ACKNOWLEDGMENT

We thank Dr. Angelika Schierhorn for mass spectrometric analysis, Achim Gärtner for N-terminal sequencing of the peptide fragments used for disulfide bond analyses, and Tanja Lisse for help with the cloning procedures. We are grateful to Gerrit Präfke and Christian Herrmann for introduction into ITC measurements and to Thomas Kiefhaber, Ariuna Bazarsuren, and Karin Berr for stimulating and helpful discussions.

REFERENCES

1. Juppner, H. (1994) *Curr. Opin. Nephrol. Hypertens. 3*, 371−378.
2. Segre, G. V., and Goldring, S. R. (1993) *Trends Endocrinol. Metab. 4*, 309−314.
3. VanRhee, A. M., and Jacobson, K. A. (1996) *Drug Dev. Res. 37*, 1−38.
4. Lee, C., Gardella, T. J., Abou-Samra, A. B., Nussbaum, S. R., Segre, G. V., Potts, J. T., Jr., Kronenberg, H. M., and Juppner, H. (1994) *Endocrinology 135*, 1488−1495.
5. Ji, T. H., Grossmann, M., and Ji, I. (1998) *J. Biol. Chem 273*, 17299−17302.

[2] This nomenclature allows a common assignment of the cysteine residues in the N-terminal domain of all class B G-protein-coupled receptors, taking into account the additional cysteine residue at the extreme N-terminus of the receptors for secretin, PACAP, and vasoactive intestinal peptide (VIP).

6. Bergwitz, C., Gardella, T. J., Flannery, M. R., Potts, J. T., Jr., Kronenberg, H. M., Goldring, S. R., and Juppner, H. (1996) *J. Biol. Chem. 271*, 26469−26472.
7. Potts, J. T., Jr., Gardella, T. J., Juppner, H., and Kronenberg, H. (1997) *Osteoporosis Int. 7* (Suppl 3), S169−S173.
8. Kronenberg, H. M., Abou-Samra, A., Bringhurst, F. R., Gardella, T. J., Jüppner, H., and Segre, G., V (1997) in *Molecular Genetics in Endocrine Disorders* (Thakker, R. V., Ed.) Chapman & Hall, London.
9. Grisshammer, R., and Tate, C. G. (1995) *Q. Rev. Biophys. 28*, 315−422.
10. Pellegrini, M., Bisello, A., Rosenblatt, M., Chorev, M., and Mierke, D. F. (1998) *Biochemistry 37*, 12737−12743.
11. Behar, V., Bisello, A., Bitan, G., Rosenblatt, M., and Chorev, M. (2000) *J. Biol. Chem. 275*, 9−17.
12. Mannstadt, M., Luck, M. D., Gardella, T. J., and Juppner, H. (1998) *J. Biol. Chem. 273*, 16890−16896.
13. Zhou, A. T., Bessalle, R., Bisello, A., Nakamoto, C., Rosenblatt, M., Suva, L. J., and Chorev, M. (1997) *Proc. Natl. Acad. Sci. U.S.A. 94*, 3644−3649.
14. Bisello, A., Adams, A. E., Mierke, D. F., Pellegrini, M., Rosenblatt, M., Suva, L. J., and Chorev, M. (1998) *J. Biol. Chem. 273*, 22498−22505.
15. Wilmen, A., Goke, B., and Goke, R. (1996) *FEBS Lett. 398*, 43−47.
16. Cao, Y. J., Gimpl, G., and Fahrenholz, F. (1995) *Biochem. Biophys. Res. Commun. 212*, 673−680.
17. Kurland, C., and Gallant, J. (1996) *Curr. Opin. Biotechnol. 7*, 489−493.
18. Brinkmann, U., Mattes, R. E., and Buckel, P. (1989) *Gene 85*, 109−114.
19. Teich, A., Lin, H. Y., Andersson, L., Meyer, S., and Neubauer, P. (1998) *J. Biotechnol. 64*, 197−210.
20. Gill, S. C., and von Hippel, P. H. (1989) *Anal. Biochem. 182*, 319−326.
21. Rivas, G., Stafford, W., and Minton, A. P. (1999) *Methods 19*, 194−212.
22. Schmid, F. X. (1989) in *Protein Structure: A Practical Approach* (Creighton, T. E., Ed.) pp 251−285, IRL Press at Oxford University, Oxford.
23. Bohm, G., Muhr, R., and Jaenicke, R. (1992) *Protein Eng. 5*, 191−195.
24. Tannhauser, T. W., Konishis, Y., and Scheraga, H. S. (1987) in *Methods in Enzymology*, pp 115−119, Academic Press, New York.
25. Wiseman, T., Williston, S., Brandts, J. F., and Lin, L. N. (1989) *Anal. Biochem. 179*, 131−137.
26. Rolz, C., Pellegrini, M., and Mierke, D. F. (1999) *Biochemistry 38*, 6397−6405.
27. Rost, B., Casadio, R., Fariselli, P., and Sander, C. (1995) *Protein Sci. 4*, 521−533.
28. Riddles, P. W., Blakeley, R. L., and Zerner, B. (1983) *Methods Enzymol. 91*, 49−60.
29. Karpf, D. B., Bambino, T., Alford, G., and Nissenson, R. A. (1991) *J. Bone Miner. Res. 6*, 173−182.
30. Graziano, M. P., Hey, P. J., Borkowski, D., Chicchi, G. G., and Strader, C. D. (1993) *Biochem. Biophys. Res. Commun. 196*, 141−146.
31. Horn, F., Bywater, R., Krause, G., Kuipers, W., Oliveira, L., Paiva, A. C., Sander, C., and Vriend, G. (1998) *Recept. Channels 5*, 305−314.
32. Rosenblatt, M., Kronenberg, H. M., and Potts, J. T., Jr. (1989) in *Endocrinology* (Saunders, Ed.) pp 848−891, DeGroot, Philadelphia.
33. Dempster, D. W., Cosman, F., Parisien, M., Shen, V., and Lindsay, R. (1993) *Endocrinol. Rev. 14*, 690−709.
34. Gardella, T. J., Luck, M. D., Jensen, G. S., Usdin, T. B., and Juppner, H. (1996) *J. Biol. Chem. 271*, 19888−19893.
35. Marston, F. A. (1986) *Biochem. J. 240*, 1−12.
36. Lilie, H., Schwarz, E., and Rudolph, R. (1998) *Curr. Opin. Biotechnol. 9*, 497−501.
37. Schrattenholz, A., Pfeiffer, S., Pejovic, V., Rudolph, R., Godovac-Zimmermann, J., and Maelicke, A. (1998) *J. Biol. Chem. 273*, 32393−32399.
38. Rudolph, R., Fischer, S., and Mattes. (1995) U.S. Patent 5.453,363.
39. Buchner, J., and Rudolph, R. (1991) *Biotechnology (N.Y.) 9*, 157−162.
40. Timasheff, S. N., and Arakawa, T. (1989) in *Protein Structure: A Practical Approach* (Creighton, T., Ed.) pp 331−336, IRL Press at Oxford University, Oxford.
41. De Bernardez, C. E., Schwarz, E., and Rudolph, R. (1999) *Methods Enzymol. 309*, 217−236.
42. Rudolph, R., Bohm, G., Lilie, H., and Jaenicke, R. (1998) in *Protein Function: A Practical Approach* (Creighton, T. E., Ed.) pp 57−99, IRL Press at Oxford University, Oxford.
43. Gardella, T. J., Wilson, A. K., Keutmann, H. T., Oberstein, R., Potts, J. T., Jr., Kronenberg, M., and Nussbaum, S. R. (1993) *Endocrinology 132*, 2024−2030.
44. Goldman, M. E., Chorev, M., Reagan, J. E., Nutt, R. F., Levy, J. J., and Rosenblatt, M. (1988) *Endocrinology 123*, 1468−1475.
45. Gardella, T. J., Juppner, H., Wilson, A. K., Keutmann, H. T., Abou-Samra, A. B., Segre, G. V., Bringhurst, F. R., Potts, J. T., Jr., Nussbaum, S. R., and Kronenberg, H. M. (1994) *Endocrinology 135*, 1186−1194.
46. Leff, P. (1995) *Trends Pharmacol. Sci. 16*, 89−97.
47. Brown, P. J., and Schonbrunn, A. (1993) *J. Biol. Chem. 268*, 6668−6676.
48. Lelianova, V. G., Davletov, B. A., Sterling, A., Rahman, M. A., Grishin, E. V., Totty, N. F., and Ushkaryov, Y. A. (1997) *J. Biol. Chem. 272*, 21504−21508.
49. Moroder, L., Romano, R., Guba, W., Mierke, D. F., Kessler, H., Delporte, C., Winand, J., and Christophe, J. (1993) *Biochemistry 32*, 13551−13559.
50. Schwyzer, R. (1986) *Biochemistry 25*, 4281−4286.
51. Beck-Sickinger, A. G. (1996) *DDT 1*, 502−513.
52. George, S. T., Ruoho, A. E., and Malbon, C. C. (1986) *J. Biol. Chem. 261*, 16559−16564.
53. Gardella, T. J., Luck, M. D., Fan, M. H., and Lee, C. (1996) *J. Biol. Chem 271*, 12820−12825.
54. Schagger, H., and von Jagow, G. (1987) *Anal. Biochem. 166*, 368−379.
55. Bisello, A., Greenberg, Z., Behar, V., Rosenblatt, M., Suva, L. J., and Chorev, M. (1996) *Biochemistry 35*, 15890−15895.

BI0001426